Elastic/Viscoplastic Constitutive Model for Fiber Reinforced Thermoplastic Composites

T. S. Gates* and C. T. Sun†
Purdue University, West Lafayette, Indiana 47907

A constitutive model to describe the elastic/viscoplastic behavior of fiber-reinforced thermoplastic composites under plane stress conditions is presented. Formulations are given for quasistatic plasticity and time-dependent viscoplasticity. Experimental procedures required to generate the necessary material constants are explained, and the experimental data is compared to the predicted behavior.

Introduction

RECENTLY, a new composite material system, graphite/thermoplastic, has been under investigation as an alternative to the common graphite/epoxy composite materials. It is expected that during both initial part fabrication and subsequent service life, the structural component made from graphite/thermoplastic will be subjected to mechanical and thermal loads that may cause the material to exceed its elastic limit and induce strains that are dependent upon loading rate.

To accurately predict this nonlinear, time-dependent material behavior, comprehensive analytical methods are required. It is the purpose of the current research to provide a foundation for the constitutive model and experimental procedures needed to characterize the elastic/viscoplastic behavior of graphite/thermoplastic composites.

Material System

The material system used in this investigation is composed of continuous AS4 graphite fibers embedded in polyether ether ketone (PEEK) matrix material. Panels of 10-ply unidirectional material were used in the experimental program. A listing of the measured material properties is given in Table 1.

Off-axis coupon test specimens were cut from the supplied panels. These specimens measured 2.5 × 23 cm and had glass/epoxy end tabs. Specimens cut from these panels were oriented such that the fiber direction was at some predetermined angle θ to the longitudinal axis of the specimen. A range of off-axis angles was selected to maximize utilization of the material and yet provide an acceptable data base for characterization of the material for θ between 0 and 90 deg.

Table 1 APC-2, AS4/PEEK material properties

Glass transition temperature $T_g = 143°C$		
	24°C	93°C
E_1, MPa	130.3×10^3	130.3×10^3
E_2, MPa	10.3×10^3	9.58×10^3
V_{12}	0.32	0.31
a_{66}	1.40	1.40
n	7.10	6.20
A, MPa^{-n}	11.6×10^{-18}	5.1×10^{-15}
K_L[a], MPa	26.90	28.60
K_R[b], MPa	1.7×10^6	3.1×10^6
m_L[a]	0.16	0.10
m_R[b]	1.03	1.05

[a]$L \Rightarrow$ loading. [b]$R \Rightarrow$ stress relaxation.

Experimental Equipment and Procedures

Uniaxial tension tests were performed on the off-axis specimens to establish the strain rate dependency effects and find the required experimental parameters. Back-to-back Micro-Measurements axial strain gauges were mounted on the specimen to measure the extensional strain (see Fig. 1).

The tension tests were performed in a hydraulically actuated MTS testing machine capable of a 22 kips maximum load. Load was applied to the specimen by using a constant head displacement rate (stroke control) that was selectable from the MTS programmable function generator. For the tension tests, the ramp function was selected to allow for approximation of a constant strain rate type of test. Periods of zero strain rate could then be applied by interrupting the ramp with a hold signal. The strain rate was found from the measured strain data. The strain measurements can be considered to be conventional or engineering strain.

An analog signal proportional to applied load and crosshead displacement was provided by the MTS signal conditioner. Nominal stress on the specimen was calculated using the load from the MTS load cell and dividing by the average test specimen cross-sectional area measured before applying any load.

A thermostatically controlled Thermotron oven was used to maintain the desired ambient temperature around the test specimen. All of the tests were conducted using isothermal conditions.

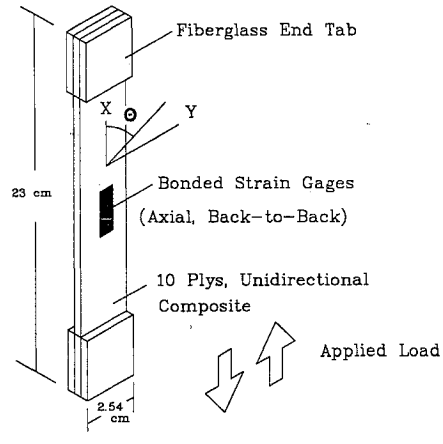

Fig. 1 Off-axis specimen.

Received Aug. 21, 1989; revision received April 16, 1990; accepted for publication April 19, 1990.

*Currently, Research Scientist, Analytical Services and Materials, Inc., NASA Langley Research Center, Hampton, Virginia 23665. Student Member AIAA.

†Professor, School of Aeronautics and Astronautics. Associate Fellow AIAA.

The four experimental parameters—strain, load, displacement and time—were recorded digitally on a PC-based data acquisition system. The PC was an AT-type clone, and the data acquisition board was a Metrabyte DASH-16. Data smoothing and conversion were performed by the software that controlled the system. The time base was generated internally from the data acquisition clock system.

A test plan was selected to give the necessary experimental information on the susceptibility of the graphite/thermoplastic material system to variable strain rate type of loading. Two sets of tests, 24 and 93°C, respectively, were performed. It was expected that this range of temperature was sufficient to demonstrate any susceptibility of the material parameters to temperature effects below glass transition. In addition to a range of temperatures, two different types of loading histories were explored.

The first type of loading used can be characterized as monotonic in nature. A single-stroke rate was selected and held constant for the entire duration of the test. Actual strain rate of the test specimen was computed based upon the measured strains.

The second type of loading used can be characterized by a variable strain rate history. Periods of constant positive or negative strain rates were applied to the specimen by selecting the appropriate stroke rates. A period of zero strain rate was applied by holding the test machine stroke rate at zero. This zero strain rate period allowed the specimen to undergo stress relaxation. During relaxation, the stress was observed to decrease at a variable rate. This stress/time behavior during relaxation can be accurately modeled as a decaying exponential function. Figure 2 is a schematic illustrating the relationships between stress/strain/time during periods of varying strain rates. A time independent or quasistatic stress/strain response is also shown on the schematic.

Because the stress/strain/time characterization of the composite in the region of developed plastic strain was of primary interest, many of the specimens were not loaded all the way to final specimen failure. Therefore, the end points on the stress/strain/time plots presented in this paper should not be interpreted as failure points.

Test specimens with fiber angles of approximately 0, 15, 30, 60, and 90 deg were used. As expected, the 0-deg specimen exhibited linear, rate-independent stress/strain behavior up to failure. The 90-deg specimens exhibited both nonlinearity and rate dependency. However, because of their relatively low failure strains, a minimum of useful information was available from the tests. Consequently, in the interest of clarity, only data from the other off axis has been presented.

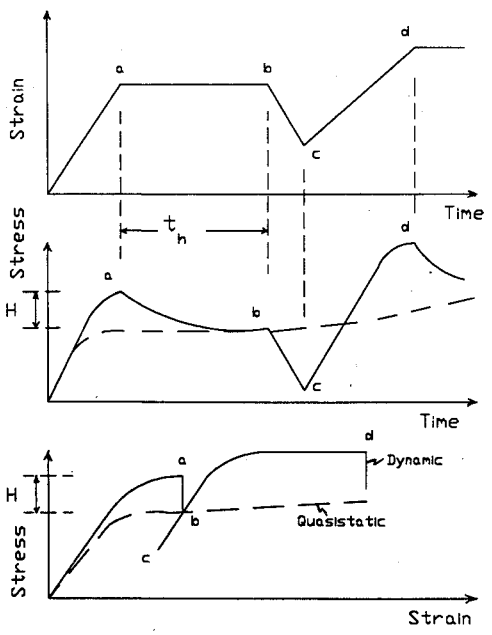

Fig. 2 Schematic illustrating the stress/strain/time relationships.

Elastic/Viscoplastic Characterization

For the unidirectional composite, the multiaxial model is used to define the tensorial relationship between stress and strain for a general state of loading. This section details the derivation of an orthotropic plate under a state of uniaxial off-axis tension loading. Working within this context, the elastic/viscoplastic constitutive equations will be developed. Based on the developed model, the time-dependent stress/strain behavior of the off-axis type of test can be predicted.

Elastic/Plastic Constitutive Relations

The basis of the viscoplastic theory presented here assumes that the instantaneous dynamic stress must be measured relative to a static stress at the same strain. This state of static stress can be represented by a quasistatic model.

In the present research effort, the elastic/plastic flow rule presented by Sun and Chen[1] is used to characterize this quasistatic response. In their paper, Sun and Chen developed a one-parameter plastic potential function to describe the nonlinear behavior of orthotropic fiber-reinforced composite materials. The one-parameter plastic potential function is given by

$$2f = \sigma_{22}^2 + 2a_{66}\sigma_{12}^2 \tag{1}$$

where 1, 2 imply the material principal directions, and a_{66} is the material constant found from off-axis tension.

The total strain increment can be decomposed into elastic and plastic strain components as

$$d\epsilon_{ij} = d\epsilon_{ij}^e + d\epsilon_{ij}^p \tag{2}$$

By using the associated flow rule, the incremental plastic strains can be written in terms of the plastic potential f as

$$d\epsilon_{ij}^p = \frac{\partial f}{\partial \sigma_{ij}} d\lambda \tag{3}$$

where $d\lambda$ is the proportionality factor.

For a state of off-axis tension, the applied stress is σ_x. Working in a Cartesian coordinate system and using coordinate transformation relations, the normal- and shear-stress components in the material principal directions are given by

$$\sigma_{11} = \sigma_x \cos^2\theta$$

$$\sigma_{22} = \sigma_x \sin^2\theta$$

$$\sigma_{12} = -\sigma_x \sin\theta \cos\theta \tag{4}$$

The effective stress and effective plastic strain increment as defined in Ref. 1 are given explicitly by

$$\bar{\sigma} = \sqrt{3f} = \left[\frac{3}{2}(\sigma_x^2 \sin^4\theta + 2a_{66}\sigma_x^2 \sin^2\theta \cos^2\theta)\right]^{1/2} \tag{5}$$

$$d\bar{\epsilon}^p\epsilon = \left[\frac{2}{3}(\sigma_x^2 \sin^4\theta + 2a_{66}\sigma_x^2 \sin^2\theta \cos^2\theta)\right]^{1/2} d\lambda \tag{6}$$

We define the quantity

$$h(\theta) \equiv \left[\frac{3}{2}(\sin^4\theta + 2a_{66} \sin^2\theta \cos^2\theta)\right]^{1/2} \tag{7}$$

We note that with the use of Eq. (7) all the terms relating the dependence of the stresses on the off-axis angle θ are collected into one function. This function also depends upon the material constant a_{66} from the potential function.

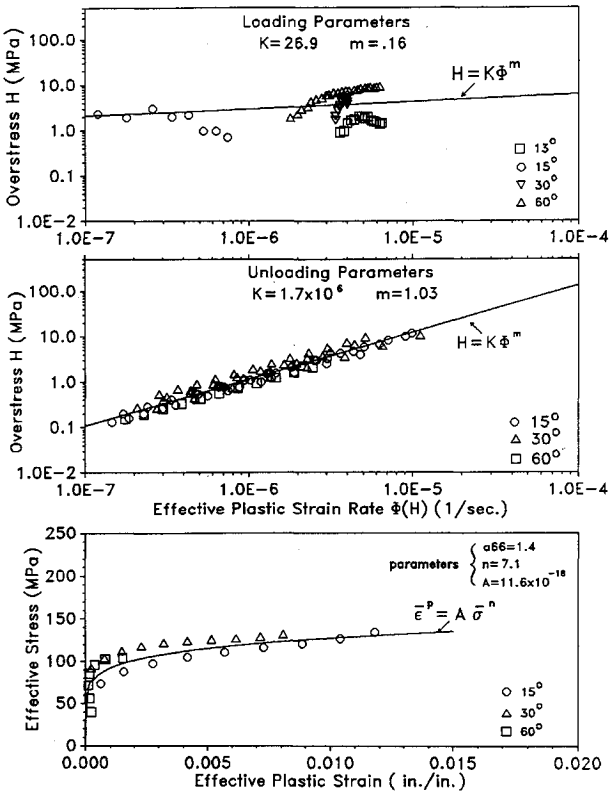

Fig. 3 Material property master curves at 24°C.

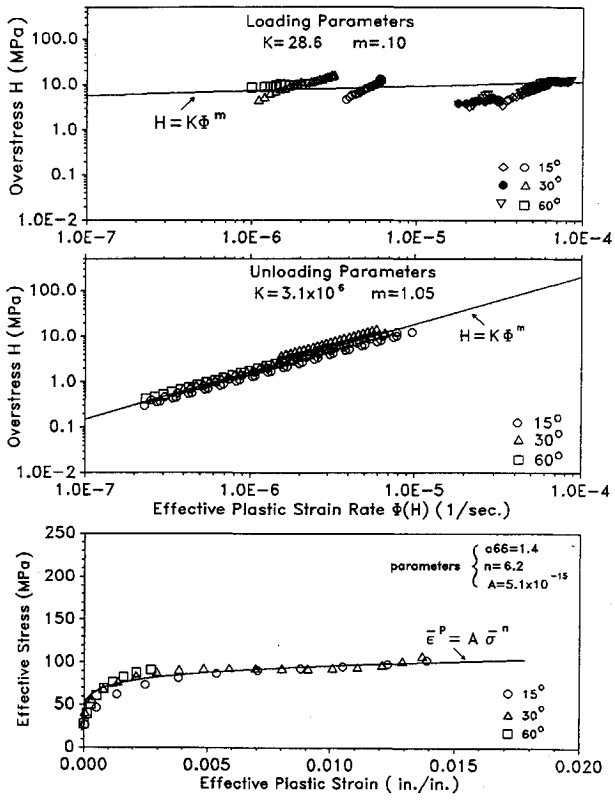

Fig. 4 Material property master curves at 93°C.

Use of Eq. (7) allows Eqs. (5) and (6) to be written as

$$\bar{\sigma} = h(\theta)\sigma_x \tag{8}$$

$$\bar{\epsilon}^p = [\epsilon_x^p / h(\theta)] \tag{9}$$

Therefore, the effective stress and effective plastic strain can be written in terms of the off-axis angle θ, the material constant a_{66}, and the axial stress and axial plastic strain, respectively.

Using simple off-axis tension specimens, the quasistatic points can be found by performing multiple relaxation events during a uniaxial tension test.[2] The quasistatic stress/strain curve can then be defined experimentally by using stress and strain values of the dynamic stress/strain test after stress relaxation has occurred. During relaxation, the stress time data can be represented by a decaying exponential function. From this representation, it is possible to find a value of stress that approximates the minimum stress reached during relaxation. This minimum value can be considered to correspond to the quasistatic stress point.

These quasistatic stress/strain curves can then be converted to an effective stress/effective plastic strain curve using the relationships given above. The material constant a_{66} that appears in the potential function is selected so that the effective stress-effective plastic strain curves for the off-axis tests collapse into a single curve. These effective stress/effective plastic strain curves are shown in Figs. 3 and 4.

Assuming that the off-axis tension specimen exhibits some plastic deformation for any value of stress greater than zero, a power law expression can be used to characterize the effective stress/effective plastic strain relation. This power law is of the form

$$\bar{\epsilon}^p = A(\bar{\sigma})^n \tag{10}$$

where A and n are material constants. In terms of the axial quantities of stress and plastic strain, and assuming that the total axial strain can be decomposed into an elastic and plastic quantity, the total quasistatic stress/strain relationship may now be given by

$$\epsilon_x = \frac{\sigma_x}{E_x} + [h(\theta)]^{n+1} A(\sigma_x)^n \tag{11}$$

In this expression, the subscript x refers to the loading direction, and the quantity E_x is the longitudinal modulus of the off-axis specimen. Equation (11) allows the quasistatic, nonlinear stress/strain relationship to be predicted for a state of uniaxial stress at any angle θ relative to the material principal directions.

Elastic/Viscoplastic Constitutive Relations

It is desired to use a formulation for anisotropic viscoplasticity that is consistent with that presented for anisotropic plasticity. In the rate-dependent constitutive relation development, we assume that the rate-dependent strain can be decomposed into an elastic and plastic component given by

$$\dot{\epsilon}_{ij} = \dot{\epsilon}_{ij}^e + \dot{\epsilon}_{ij}^p \tag{12}$$

where the overdot implies a derivative with respect to time, and $\dot{\epsilon}_{ij}^p$, $\dot{\epsilon}_{ij}^e$ are the plastic and elastic strain rate, respectively.

It is assumed that the dynamic loading surface is everywhere parallel to the quasistatic yield surface. Because of this fact, the normals of their respective potential functions will coincide for any points on the two surfaces connected by a straight line extending from the center of the yield surface. Therefore, we let the potential function be given by

$$2f = \sigma_{22}^2 + 2a_{66}\sigma_{12}^2$$

which implies that the one-parameter potential function used to describe the quasistatic yield surface may also be used to define the dynamic potential function.

Using the associated flow rule, the time rate of change of the plastic strains can be written in terms of f as

$$\dot{\epsilon}_{ij}^p = \frac{\partial f}{\partial \sigma_{ij}} \dot{\lambda}' \tag{13}$$

where $\dot{\lambda}'$ implies a proportionality factor used to bring in the time rate of change of stress. As in the quasistatic case, the ability to account for anisotropy is handled by the potential function. The time rate of change of plastic work per unit volume is

$$\dot{W}^p = \sigma_{ij}\dot{\epsilon}_{ij} \tag{14}$$

The effective plastic strain rate $\bar{\epsilon}^p$ is defined through the relation

$$\dot{W}^p = \bar{\sigma}\dot{\bar{\epsilon}}^p \tag{15}$$

So, using Eqs. (13) and (15) gives

$$\dot{\lambda}' = (3/2)/(1/\bar{\sigma})\dot{\bar{\epsilon}}^p \tag{16}$$

The basis for the time-dependent or viscous constitutive model selected to analyze the rate-dependent nature of graphite/thermoplastics has its origins in a theory set forth by Malvern[3] in his paper on wave propagation. Malvern proposed that a viscoplastic component of strain exists during high strain rate conditions. He stated that this viscoplastic strain can be found by taking "the excess of the instantaneous stress over the stress at the same strain in a static test." This difference in stress values is commonly referred to as overstress.

Sixteen years after this paper by Malvern, Perzyna[4] also presented Malvern's theory in a comprehensive monograph on viscoplasticity. In this work, both uniaxial and multiaxial derivations were outlined for applications to viscous behavior of metals. As defined by Perzyna, an "elastic/viscoplastic" material shows viscous properties in the plastic region only. This latter case will be the only one considered in this research effort.

In their book on viscoplasticity, Cristescu and Suliciu[5] also discussed using overstress to determine the plastic strain rate component. They presented several alternative forms for the overstress function and developed the general strain rate expressions necessary for construction of the rate-dependent constitutive equations.

Within the last 10 years, the idea of an overstress function and its relationship to plastic strain rate has been explored by Eisenberg and Yen.[6,7] In several papers on the subject, they derived both the uniaxial and multiaxial flow laws for strain-hardening metallics alloys such as modern aluminum alloys. They noted that the theoretical lower bound of the rate-dependent stress/strain curve is found by assuming quasistatic behavior. They observed that this quasistatic level can be found by allowing the material to relax after reaching some stress level in a rate-dependent stress/strain test.

The use of the overstress function to describe the rate-dependent plastic strain has been largely limited to applications to isotropic metallic alloys. However, Sutcu and Krempl[8] used the concept of overstress to describe viscoplasticity in an anisotropic, directionally solidified alloy. The theory as presented by Sutcu and Krempl does not allow plasticity and creep to be represented by separate constitutive equations and does not employ the concepts of a yield surface and associated loading and unloading conditions.

In the current research, we state the relationship between plastic strain rate and overstress by letting

$$\dot{\bar{\epsilon}}^p = \langle \Phi(H) \rangle \tag{17}$$

where H is the overstress and $\Phi(H)$ implies some function dependent on overstress. The brackets in this expression imply

$$\langle \Phi(H) \rangle = \begin{cases} \Phi(H) & \text{if } H > 0 \text{ (loading)} \\ 0 & \text{if } H \leq 0 \text{ (unloading)} \end{cases}$$

From these relationships, we can write the proportionality factor as

$$\dot{\lambda}' = (3/2)(1/\bar{\sigma})\langle \Phi(H) \rangle \tag{18}$$

Letting $\gamma = (3/2)\ (1/\bar{\sigma})$, the flow rule can be written in the form

$$\dot{\epsilon}^p_{ij} = \gamma \frac{\partial f}{\partial \sigma_{ij}} \langle \Phi(H) \rangle \tag{19}$$

The overstress (H) can be considered a scalar quantity that relates the quasistatic stress to the dynamic or instantaneous stress at the same strain level. The quasistatic stress is found by using the previously defined time-independent elastic/plastic relations, while the dynamic stress is the stress resulting from the time-dependent material behavior. The quasistatic stress/strain curve may be interpreted as a sequence of equilibrium states such that plastic flow occurs at finite loading rates when the flow condition is satisfied. Therefore, the quantity H vanishes in the limit as σ_{ij} approaches the quasistatic stress. Figure 2 illustrates these relationships.

The flow surface defined by the one-parameter potential function is regular and convex. In addition, Eq. (19) implies that the plastic strain rate is always directed along a normal to the subsequent dynamic loading surface. This dynamic loading surface is located some distance away from the quasistatic hardening surface. This distance is specified by the amount of overstress occurring at a given time and for a given strain. The overstress then represents a driving potential for viscoplastic strain.

For off-axis tension the effective plastic strain rate is given by

$$\dot{\bar{\epsilon}}^p = \left[\frac{2}{3}(\sigma_x^2 \sin^4\theta + 2a_{66}\sigma_x^2 \sin^2\theta \cos^2\theta)\right]^{1/2} \dot{\lambda}' \tag{20}$$

As in the elastic/plastic case, the dependency upon θ and a_{66} can be collected into the expression $h(\theta)$. Using $h(\theta)$, we have effective stresses given by

$$\bar{\sigma} = h(\theta)\sigma_x, \qquad \sigma_x \equiv \text{dynamic axial stress} \tag{21a}$$

$$\bar{\sigma}^* = h(\theta)\sigma_x^*, \qquad \sigma_x^* \equiv \text{quasistatic axial stress} \tag{21b}$$

where the quasistatic stress is found from Eq. (11). Defining an expression for effective plastic strain rate

$$\dot{\bar{\epsilon}}^p = \dot{\epsilon}_x^p \frac{1}{h(\theta)} \tag{22}$$

allows Eq. (18) to be written as

$$\dot{\lambda}' = \frac{3}{2}\frac{1}{h(\theta)^2\sigma_x}\dot{\epsilon}_x^p \tag{23}$$

This implies that

$$\gamma\langle \Phi(H) \rangle = \frac{3}{2}\frac{1}{h(\theta)^2}\frac{1}{\sigma_x}\dot{\epsilon}_x^p \tag{24}$$

and the potential function gives the gradient

$$\frac{\partial f}{\partial \sigma_x} = \sigma_x \frac{2}{3} h(\theta)^2 = \frac{2}{3} h(\theta)\bar{\sigma} \tag{25}$$

As shown previously, the plastic strain rate term is defined using the overstress function. We let the overstress be defined by

$$H = \bar{\sigma} - \bar{\sigma}^* \tag{26}$$

Using the relations given by Eq. (21), we have

$$H = h(\theta)(\sigma_x - \sigma_x^*) = h(\theta)\, H_x \tag{27}$$

For off-axis tension and using notation similar to Cristescu and Suliciu[5] and Peryzna,[4] the brackets in Eq. (17) imply

$$<\Phi> = \begin{cases} \Phi \text{ if } \sigma_x > g(\epsilon_x) \\ 0 \text{ if } \sigma_x \leq g(\epsilon_x) \end{cases} \tag{28}$$

If we let $g(\epsilon_x)$ imply a function based upon total axial strain, and noting the overstress relation in Eq. (26), the function $g(\epsilon_x)$ can now be selected to be $g(\epsilon_x) \equiv \sigma_x^*$, where the quasistatic axial stress σ_x^* can be found by solving the quasistatic stress/strain relationship, e.g.,

$$\epsilon_x = \frac{\sigma_x^*}{E_x} + (h(\theta))^{n+1} A\, (\sigma_x^*)^n \tag{29}$$

The axial plastic strain rate for off-axis tension may now be written as

$$\frac{1}{h(\theta)}\, \dot{\epsilon}_x^p = <\Phi[h(\theta) H_x]> \tag{30}$$

Based upon the observed form of the experimental data, a power law expression was selected to represent the explicit relationship between effective plastic strain rate and overstress. The form of this power law is given by

$$\bar{\dot{\epsilon}}^p = \Phi(H) = \left(\frac{H}{K}\right)^{1/m} \tag{31}$$

where K and m are material constants found from the test data. After careful observation of the material behavior under different loading conditions, it was decided to separate the constants found from the relaxation condition from those from the loading condition. Therefore, we have,

$$K_R,\ m_R \Rightarrow \text{stress relaxation}$$

$$K_L,\ m_L \Rightarrow \text{loading case}$$

During stress relaxation the stress is decreasing (i.e., stress rate is negative). For a stress above the quasistatic level, a plastic strain rate term may exist. Material constants can be found to help define this plastic strain rate. Performing stress relaxation is a direct way of arriving at these parameters.

As noted before, the stress during a relaxation event appears to decay in an exponential manner. The asymptotic values of the absolute change in stress during relaxation can be used to determine the overstress experimentally.

We also note that during relaxation, $\dot{\epsilon}_x = 0$, which gives

$$\dot{\epsilon}_x^p = -\dot{\epsilon}_x^e = -(\dot{\sigma}_x / E_x)$$

Therefore, by differentiating a decaying exponential fit to the stress/time curve with respect to time, the term $\dot{\sigma}_x$ can be found.

Using the relaxation test data from all of the relaxation events and the $h(\theta)$ expression, overstress (H) and effective plastic strain rate for several test angles θ can be plotted together on a single graph. As in the case of the effective stress/effective plastic strain plots, the data will tend to collapse into a single curve if the proper value of a_{66} is selected. This single curve, or "master curve," gives the necessary information to determine the relationship between measured overstress and the plastic strain rate. Figures 2 and 3 show these curves for graphite/thermoplastic at 24°C and 93°C. It should be noted that the material constant a_{66} that is used to define this master curve is the same value that was used in the quasistatic model. The flow rate for the stress relaxation case is then given by Eq. (31) where K_R and m_R are the power law parameters.

When the stress is increasing (i.e., the stress rate is positive) or is neither increasing or decreasing (i.e., zero stress rate), the material is considered to be in a state of loading. As in the stress relaxation case, the relationship between measured overstress and plastic strain rate can be determined by using experimentally measured quantities and Eq. (31).

An off-axis tension test performed by using a positive constant strain rate type of loading can be used to determine the loading parameters. The overstress at any given instant during this test is found by simply measuring the difference between the dynamic and quasistatic stress values for a given strain.

For the case of monotonically increasing strain, the applied strain rate is found from the slope of the strain/time data. This applied strain rate is considered to be the total strain rate composed of the elastic and plastic strain rate components. Differentiating the stress/time curve once with respect to time, the stress rate is determined. Dividing this stress rate by the axial elastic modulus will define the elastic strain rate term. Therefore, the plastic strain rate term is found by using these two measured strain rates and Eq. (12).

As in the unloading case, once H_x and $\dot{\epsilon}_x^p$ are known, the overstress effective plastic strain rate can be plotted against each other on the same graph for any off-axis angle θ. Figures 3 and 4 show these curves for graphite/thermoplastic at room temperature and 93°C. As before, a power law is used to give a linear representation to this data when plotted on a log-log scale. This allows the determination of the constants K_L and m_L.

Using the expression in Eq. (31), we can form an expanded expression for the effective plastic strain rate:

$$\bar{\dot{\epsilon}}^p = \Phi[h(\theta) H_x] = \left[h(\theta)\frac{H_x}{K}\right]^{1/m} \tag{32}$$

So, using the above relationships we can expand further to obtain

$$\dot{\epsilon}_x^p = [h(\theta)]^{1+(1/m)} \left(\frac{1}{K}\right)^{1/m} (\sigma_x - \sigma_x^*)^{1/m} \tag{33}$$

Collecting terms, we let

$$\beta = \beta(\theta, a_{66}, m, K) = [h(\theta)]^{1+(1/m)} \left(\frac{1}{K}\right)^{1/m} \tag{34}$$

This gives an expression for the plastic strain rate in off-axis tension:

$$\dot{\epsilon}_x^p = \Phi(H_x) = \beta(\sigma_x - \sigma_x^*)^{1/m} \tag{35}$$

Adding to this the expression for the elastic strain rate gives the constitutive equation

$$\dot{\epsilon}_x = \frac{\dot{\sigma}_x}{E_x} + \beta(\sigma_x - \sigma_x^*)^{1/m} \tag{36}$$

This relationship can be considered as the uniaxial flow rate for an off-axis orthotropic elastic/viscoplastic fiber-reinforced composite. The expression is in the form of a first-order nonlinear ordinary differential equation (ODE) with respect to time. Depending on the desired results, this ODE can be solved for stress or strain by providing a stress rate or strain rate, respectively. It should be noted that the ODE is coupled to the nonlinear expression for quasistatic stress/strain through the use of σ_x^*.

Off-Axis Tension Test Verification

The first-order nonlinear ordinary differential equation used to describe the uniaxial flow rate for elastic/viscoplastic composites [Eq. (36)] can be solved numerically using any

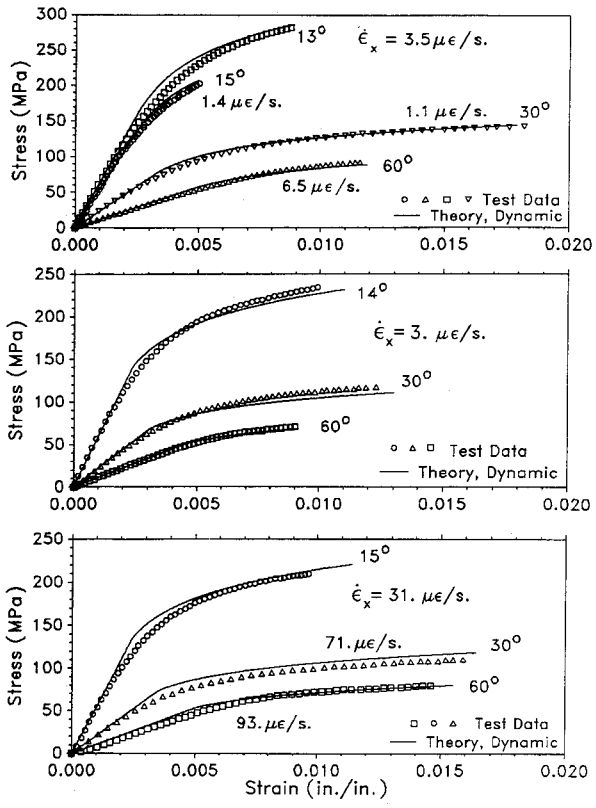

Fig. 5 Monotonic off-axis tension; test theory.

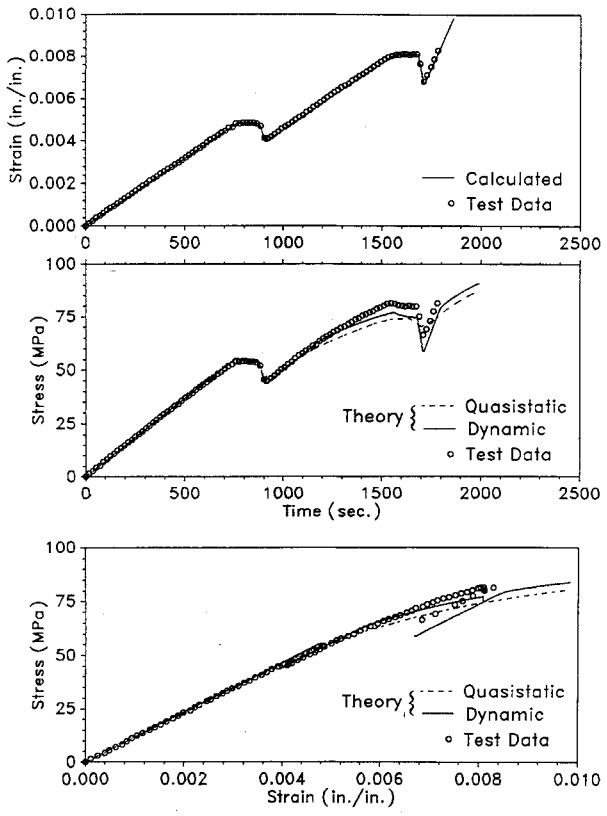

Fig. 7 Variable rate off-axis tension; test theory, 60 deg at 24°C.

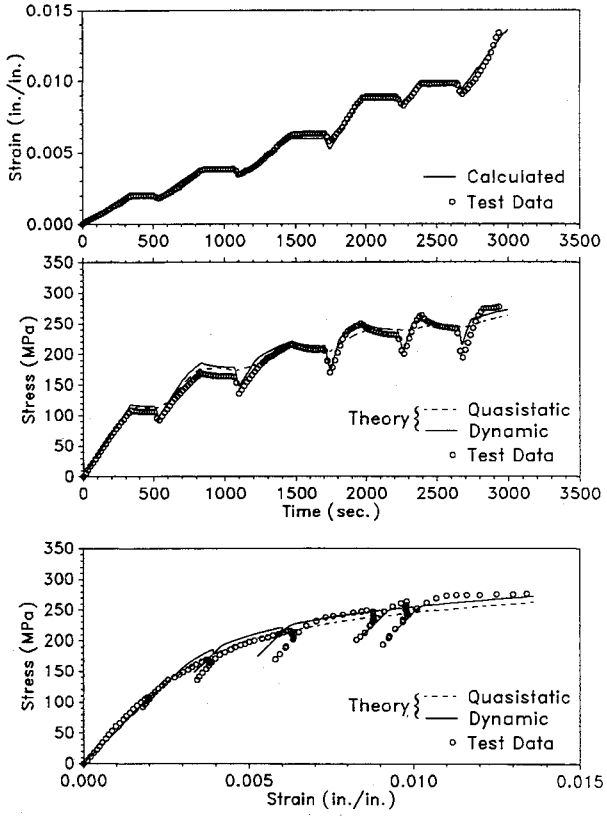

Fig. 6 Variable rate off-axis tension; test theory, 15 deg at 24°C.

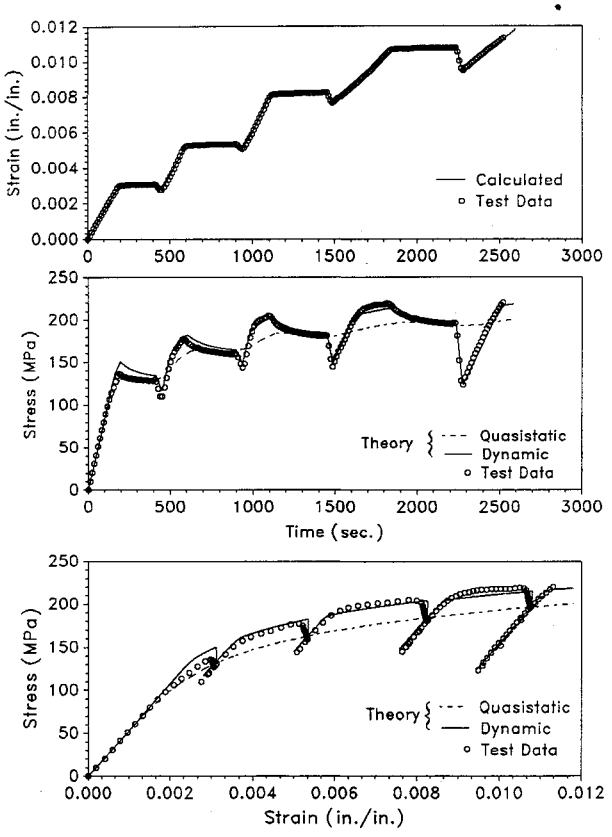

Fig. 8 Variable rate off-axis tension; test theory, 15 deg at 93°C.

number of different techniques. The technique used here was to implement the Runge-Kutta fourth-order solution algorithm on a microprocessor based personal computer.

Implicit in the ODE given by Eq. (36) is the nonlinear algebraic expression, Eq. (29), relating plastic strain and quasistatic stress. The algorithm used to solve numerically for the roots of this polynomial is a form of Newton's method.

Predictions of the stress/strain response of representative off-axis specimens are shown in Figs. 4–8. The exact strain rates, as measured experimentally, along with the measured

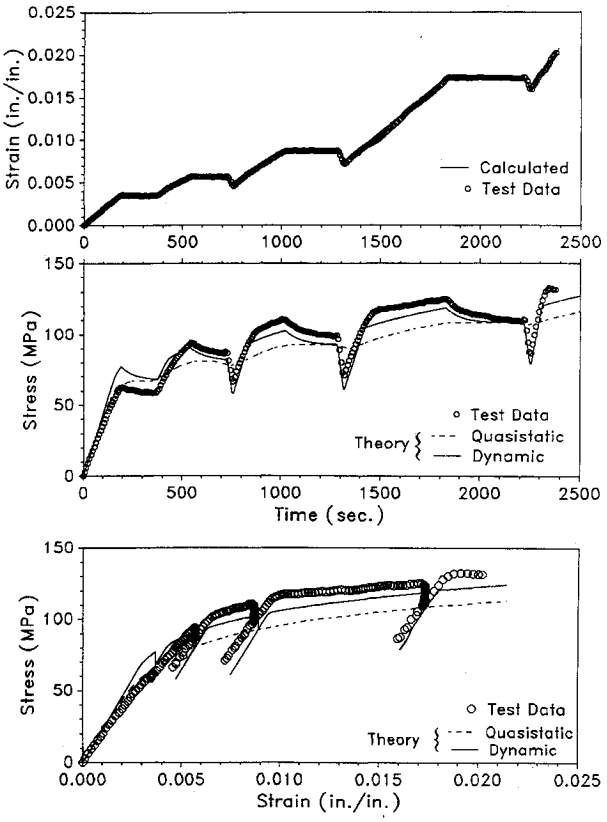

Fig. 9 Variable rate off-axis tension; test theory, 30 deg at 93°C.

material constants, are provided as input into a FORTRAN program. The program provides a numerical solution to Eqs. (29) and (36) to predict the quasistatic and dynamic behavior.

Regarding the accuracy of the theoretical predictions, two questions need to be answered. First, what is the magnitude of the error between test and theory? Second, does the theoretical model capture the correct form of the material response during complex events such as yielding and relaxation? By comparing the theoretical predictions to the test data for the stress/strain time behavior of the off-axis tests, these questions are answered, and several conclusions can be drawn.

To answer the first question, it is necessary to compare test theory as shown on Figs. 4–8. In general, it can be seen from these figures that the magnitude of the error between test and theory is within an acceptable range for both the monotonic and variable rate tests.

The second question may also be answered by comparing test versus theory on Figs. 5–9. For the monotonic rate tests, an important feature to model accurately is the transition from elastic to plastic strains. It can be seen from the monotonic rate figures that the prediction of this transition region or "knee" in the stress/time and stress/strain curves has some error associated with it for the lower angles such as 15 deg. However, despite this error, the theory does a good job of predicting the amount of total plastic strain developed during loading. For higher angles such as 30 and 60 deg, the total stress/time or stress/strain curve is represented well.

For the variable rate loading, the ability of the theory to accurately portray the form of the material response during periods of stress relaxation, elastic unloading, and rate-dependent elastic/plastic loading is of high importance to ensure confidence in the analytical model. Comparing test data to the predicted dynamic and quasistatic response on Figs. 5 through 9 shows that the elastic/viscoplastic model does a good job of characterizing the form of the data.

Conclusions

A simple constitutive model for the elastic/viscoplastic behavior of orthotropic graphite/thermoplastic composites is presented. The model includes the effects of material nonlinearity and elevated temperature. In addition, the material constants required for the model can easily be found from tension tests on off-axis unidirectional coupon specimens. The material constants found from these tests can then be used in the constitutive model to predict the stress/strain/time behavior of the material under general loading.

With this model, viscous effects such as creep and relaxation can be accounted for and predicted. Incorporating the constitutive equations into lamination theory will allow the ability to predict the stress/strain response of a laminate undergoing a complicated strain rate or stress rate history.

Acknowledgment

This work was supported by the National Science Foundation under Grant CDR 8803017 to the Engineering Research Center for Intelligent Manufacturing Systems, Purdue University, West Lafayette, Indiana.

References

[1]Sun, C. T., and Chen, J. L., "A Simple Flow Rule for Characterizing Nonlinear Behavior of Fiber Composites," *Journal of Composite Materials,* Vol. 23, No. 10, 1989, pp. 1009–1020.

[2]Yen, C. F., Wang, K. F., and Hsiao, W. C., "An Experimental Study of the Uniaxial Rate-Dependent Behavior of Type 304 Stainless Steel at Room Temperature," Spring Conference on Experimental Mechanics, Society for Experimental Mechanics, New Orleans, LA, June 8-13, 1986.

[3]Malvern, L. E., "The Propagation of Longitudinal Waves of Plastic Deformation in a Bar of Material Exhibiting a Strain-Rate Effect," *ASME Journal of Applied Mechanics,* Vol. 18, 1951, pp. 203–208.

[4]Perzyna, P., "Fundamental Problems in Viscoplasticity," *Advances in Applied Mechanics,* Vol. 9, 1966, pp. 244–377.

[5]Cristescu, N., and Suliciu, L., *Viscoplasticity,* Martinus Nijhoff, Hague, 1982.

[6]Eisenberg, M. A., and Yen, C. F., "A Theory of Multiaxial Anisotropic Viscoplasticity," *ASME Journal of Applied Mechanics,* Vol. 48, June 1981, pp. 276–284.

[7]Eisenberg, M. A., and Yen, C. F. "The Anisotropic Deformation of Yield Surfaces," American Society of Mechanical Engineers, Winter Meeting, New Orleans, Dec. 9–14, 1984.

[8]Sutcu, M., and Krempl, E., "A Simplified Orthotropic Formulation of the Viscoplasticity Theory Based on Overstress," NASA Conference on Nonlinear Constitutive Relations for High Temperature Applications, Pub. 10010, Akron, OH, June 11–13, 1986, pp. 89–95.